KU Leuven
Department of Mechanical Engineering
Celestijnenlaan 300 - box 2420
B-3001 Heverlee (Belgium)

Proceedings of

ISMA2020

International Conference on

Noise and Vibration Engineering

USD2020

International Conference on

Uncertainty in Structural Dynamics

7 to 9 September, 2020
Editors: W. Desmet, B. Pluymers, D. Moens, S. Vandemaele.

Proceedings of

ISMA2020

International Conference on

Noise and Vibration Engineering

USD2020

International Conference on

Uncertainty in Structural Dynamics

Leuven
7 to 9 September, 2020

Organising Committee:

Prof. Dr. ir. W. Desmet,	*ISMA Conference Chairman*
Dr. ir. B. Pluymers,	*ISMA Conference Chairman*
Prof. Dr. ir. P. Sas,	*ISMA Honorary Chairman*
Prof. Dr. ir. D. Moens,	*USD Conference Chairman*
Prof. Dr. ir. D. Vandepitte,	*Programme Chairman*
Prof. Dr. ir. W. De Roeck,	*Conference Programme*
Prof. Dr. ir. K. Gryllias,	*Conference Programme*
ir. S. Vanpaemel,	*Conference Manager*
ir. R. Adduci,	*Technical Manager*
Mrs. L. Notré,	*Conference Secretary*
ir. S. Vandemaele,	*Conference Proceedings and database*
ir. J. Kersschot,	*Exhibition*
ir. A. Angeli,	*Public Relations*
ing. O. Van Dessel,	*Social Events*
ir. S. Ahsani,	*Webmaster*

Organised by:

KU Leuven – Department of Mechanical Engineering
Celestijnenlaan 300 - box 2420
B-3001 Heverlee (Belgium)

ISBN 9789082893113

ISMA2020 PAPERS

AVC

Session Active Vibration Control

AE

Session Aero-Elasticity

AA

Session Aeroacoustics and flow noise

CAM

Session Characterisation, design and optimisation of vibro-acoustic materials and structures

CMRM

Session Condition monitoring of rotating machinery

D

Session Damping

DT

Session Dynamic testing: methods and instrumentation

JOINT

Session Dynamics of Joints

RMD

Session Dynamics of Rotating Machinery

CIV

Session Dynamics of civil structures

INV

Session Inverse Methods - Load Identification

MHF

Session Medium and High Frequency Techniques

MTC

Session Modal testing: methods and case studies

MOR

Session Model Order Reduction

MU

Session Model Update

MB

Session Multi-body dynamics and control

NL

Session Non-linearities: identification and modelling

OMCV

Session Optical Methods and Computer Vision for Vibration Engineering

PBNV2

Session Pass by noise

PER

Session Periodic structures and metamaterials

RAIL

Session Railway dynamics and ground vibrations

SD

Session Structural dynamics: methods and case studies

SHM

Session Structural health monitoring (Structures)

SC

Session Substructuring and Coupling

TVD

Session Tuned Vibration Absorbers and Dampers

NVH

Session Vehicle noise and vibration (NVH)

VAM

Session Vibro-acoustic modelling and prediction

WIND

Session Wind turbine dynamics

USD2020 PAPERS

USDUIQ

Session USD - Uncertainty Identification and Quantification

USDMP

Session USD - Uncertainty modelling and propagation

USDA

Session USD – Applications

Estimation of time-varying forces loading the vane in balanced vane pumps

M. Battarra, E. Mucchi
University of Ferrara, Department of Engineering,
Via G. Saragat 1, 44121, Ferrara (FE), Italy

Abstract

The present study proposes an analytical methodology to estimate the variable loads applied to the vanes of balanced vane pumps. The dissertation is adopted to detail the nature of the different time-varying excitations that load the machine and to define their analytical calculation on the basis of vane geometry, cam ring profile and working conditions. A comprehensive overview of the mutual interconnections between time-varying loads and the pump design is provided by means of a parametric study involving vane thickness, tip radius and cam ring shape. Admissibility of the pump geometry is verified throughout the entire study. The results show that the vane tip radius affects both the inertial forces and the under-vane pressure load by its influence on the vane radial motion. Concurrently, the vane thickness acts as a gain factor with respect to the magnitude of the under-vane pressure load. Despite not altering the kinematic vane motion, effects on the inertial forces are recognized due vane mass changing related to thickness variation.

1 Introduction

Balanced vane pumps are positive displacement machines nowadays adopted in high performance lubrication systems. Their broad application, in particular in automotive auxiliary systems, is promoted by their features of high power over weight ratios and suitable NVH performances. Nonetheless, this set of satisfactory characteristics is counterbalanced by a higher level of mechanical complexity with respect to other common volumetric pumps.

This latter aspect is probably one of the main reasons why their spread has been delayed until the last decades. As a matter of fact, volumetric pumps have represented a thriving research field since the early '40s, but the attention was mainly focused on different positive displacement machine typologies [1, 2, 3]. Several studies have been devoted to external gear, gerotor and crescent pumps with the purpose to model their performance [4, 5], their dynamic behavior [6] or their tribology [7]. The extensiveness of the studies on these families of pumps is well described by the review provided by Rundo M. in [8]. Concurrently, remarkable works related to axial piston pumps [9, 10] as well as referring to variable displacement vane pumps [11, 12] have been promoted by the research community. The predominance of these machines with respect to balanced vane pumps is recognized also in one of the most relevant book on the theory of volumetric pumps and motors [13].

Despite the trend outlined by classical studies, a growing interest related to balanced vane pumps is nowadays recognized in the specialized literature. One of the first works on this subject pertains to Hattori K. et al. [14], who proposed a numerical model to analyze the delivery pressure ripple in balanced vane pumps adopted in power steering systems. The authors provided a first insight on the relevance of the cam ring profile and the concept was further investigated by Cho M. et al. in [15], where the possibility of vane jumping phenomena was firstly considered. The fundamental role played by vane geometry and cam ring shape has been further investigated by Inaguma Y. et al. in [16] by analyzing their influence on the friction torque and the mechanical efficiency of the machine. The kinematic relationship between vane parameters and cam ring profile has been finally defined analytically in the works by Battarra et al. [17, 18], where the authors provided equations for checking the vane geometry admissibility and the theoretical flow ripple generated by the pump design parameters.

Within this context, all the analyzed studies recognize a fundamental working principle of balanced vane pumps. During operational conditions, the machine rotation causes the radial displacement of the vanes producing the pumping action, which itself enhances the vane radial motion. As a result, the vanes become guided by time-varying and working condition dependent loads that are the major responsible for the NVH behavior of the pump. In this context, the present work defines the nature of the different time-varying excitations that load the machine and details their analytical calculation on the basis of the machine design characteristics. The described purpose is fulfilled on the basis of the kinetostatic approach, which represents a common starting point for determining the dynamic behavior of mechanical systems and components [19, 20]. The dissertation starts with the analytical definition of the radial dynamics of the vanes, representing the main responsible for the machine vibration and the generated noise. Based on the assumption that the vane radial motion is the result of the superposition between the vane kinematic motion and the dynamic oscillation, the proposed analysis deepens the characteristics of the former contribution. Within this framework, the results of the kinematic analysis are adopted to define the centrifugal force loading the vane center of gravity and the kinematic pressure force generated within the under-vane pockets. The proposed dissertation provides analytical formulas estimating the variable forces loading the pump in kinetostatic conditions. As a matter of fact, these loads typically represent the reference terms for the structural design of the machine. In addition, such forces stand at the basis of the dynamic behavior of the vanes and consequently they are commonly recognized as major responsible for the behavior of the entire machine itself. Within this context, the provided dissertation is specifically focused on making explicit the mutual correlation between the pump geometry and the generated loads, by detailing the latter with respect to the main machine geometrical parameters, i.e. vane length, vane thickness, tip radius and cam ring profile.

The capabilities of the proposed analysis are highlighted by means of a parametric study, which is based on the vane geometry admissibility described in Ref. [17]. The results show that, given the cam ring profile, the vane tip radius influences the vane radial motion and consequently affects both the centrifugal force loading the vane center of gravity and the under-vane pressure load. Concurrently, the vane thickness acts as a gain factor with respect to the magnitude of the under-vane pressure load. In addition, despite not altering the motion of the vane, it varies the vane mass and consequently affect the inertial forces. Finally, the shape of the cam ring profile is shown to further affect both the considered loads, due to its influence on the derivatives of the vane radial displacement.

The following Section describes the working principle behind balanced vane pumps, while Section 3 details the theoretical dissertation developed to estimate the time varying loads applied to the vane. Section 4 defines the parametric study carried out to evaluate the capabilities of the analytical formulation and provides a critical discussion on the achieved results. Eventually, last Section is devoted to concluding remarks.

2 Pump Description

The current Section describes the fundamental elements constituting a balanced vane pump together with the pump working principle. A specific focus on the existing analogy between such machines and the cam-follower mechanism is also provided.

Based on the conceptual scheme reported in Fig. 1, three main components define the pump mechanism: the external stator, namely the cam ring, the internal rotor and the vanes. Each vane slides along a dedicated channel that extends itself radially within the rotor. Such a component is responsible for displacing the vanes from the inlet side to the outlet one. Throughout this process, the vanes are capable to trap the oil inside the pockets formed between consecutive vanes, namely the displaced chambers. During this displacing action, the distinctive cam ring profile causes the cyclic expansion and compression of the pockets, resulting in the peculiar pumping phenomenon. As a typical drawback in volumetric machines, this operating principle produces flow rate and pressure oscillations, as well as self-excited vibrations of the vanes. This latter aspect, in particular, is further enhanced by the displacing action of the under-vane pockets. As a matter of fact, part of the oil is trapped from the suction chamber by the pockets that are formed under the vanes, namely the

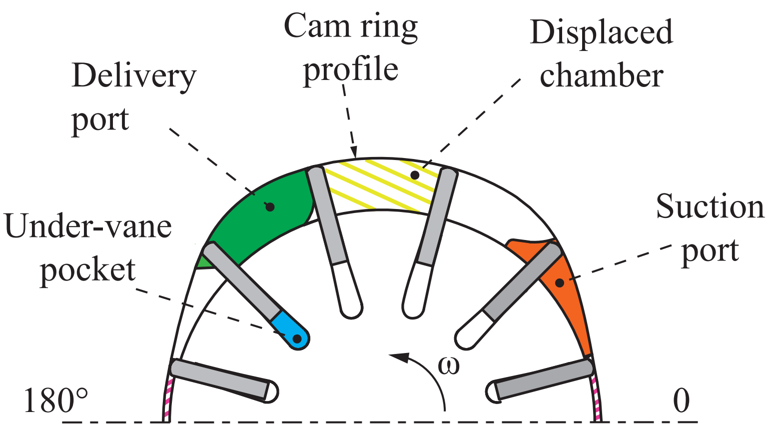

Figure 1: Main elements constituting a balanced vane pump

under-vane pockets. Their contribution to the pumping phenomenon is naturally produced by the radial movement of the vanes and they assume a relevant role with respect to the definition of the vane dynamics.

The detailed operating principle is repeated twice per revolution, since the whole pump is constituted by two identical mechanisms, which are symmetrical with respect to the axis of rotation. The described components are generally packed by two lateral plates adopted to provide the axial sealing. For the sake of completeness, it is worth noting that the complete machine includes several additional parts that are mandatory to guarantee the correct and safe functioning of the machine. However, despite their practical relevance, they do not define the pump basic characteristics and therefore their description is omitted being out of the scope of the present study.

Based on the described operating principle, it is straightforward to observe that the machine dynamics is mainly governed by the shape of the cam ring and its interaction with the sliding vanes. Within this context, the external stator can be considered as a disk cam, fixed to the external frame, while the rotating followers are constituted by the vanes. In this description, a mandatory component for the correct behavior of the mechanism is missing, i.e. the springs pushing the followers against the cam. In the framework of balanced vane pumps, this fundamental task is fulfilled by the superposition of the centrifugal force generated by the vane rotation and the pressure load produced within the under vane pockets. It is therefore clear that the vane radial dynamics is mainly governed by these two contributions, which needs to be accurately balanced in order to avoid undesired phenomena such as excessive contact forces between vane tip and cam ring as well as vane tip detachments.

The depicted scenario demonstrates the relevance for the improvement of the design process to correlate both cam ring shape and vane geometry to the variable loads applied to the vane. In this context, an analytical formulation represents a powerful tool to provide theoretical strength to design choices that are often based on the experience.

3 Analytical definition of the radial loads

The present Section details the analytical dissertation developed to compute the time-varying radial forces applied to the vanes in reference to the main pump design parameters. In agreement with the working principle described in Section 2, Fig. 2 depicts a generic vane rotating counterclockwise and three main external loads influencing its radial motion: pressure force f_p, centrifugal force f_c and reaction force f_r representing the contact force between the vane tip and the cam ring profile. By considering r_G as the instantaneous radial position of the vane center of gravity, the vane radial dynamics appears to be governed by the following equation:

$$m\ddot{r}_G + c\dot{r}_G + \cos(\beta)\, f_r = f_c + f_p \tag{1}$$

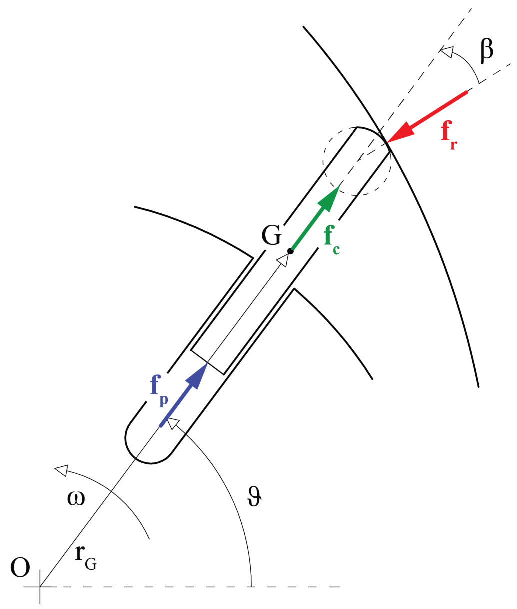

Figure 2: Schematic of the radial loads applied to the vane

where m is the vane mass, β is the pressure angle while c is the damping coefficient accounting for both structural and viscous damping. By assuming that:

$$r_G = \bar{r}_G + \tilde{r}_G \tag{2}$$

where $\bar{r}_G$ represents the kinematic component of the motion while $\tilde{r}_G$ is the oscillating term with mean value equal to zero, Eq. 1 may be further rearranged as:

$$m\left(\ddot{\bar{r}}_G + \ddot{\tilde{r}}_G\right) + c\left(\dot{\bar{r}}_G + \dot{\tilde{r}}_G\right) + \cos\left(\beta\right) f_r = f_c + f_p \tag{3}$$

where ω is the pump working speed, which may be considered as a constant for the purpose of the present study. Since the pump kinematics is exclusively defined by the geometry of the mechanism and the operating conditions, the related terms may be gathered together on the right side of Eq. 3:

$$m\ddot{\tilde{r}}_G + c\dot{\tilde{r}}_G + \cos\left(\beta\right) f_r = f_c + f_p - m\ddot{\bar{r}}_G - c\dot{\bar{r}}_G \tag{4}$$

Equation 4 clarifies the relevance of the under-vane pressure force and the centrifugal force, as well as the importance connected to a full knowledge of the machine kinematics. As a matter of fact, these three terms constitute the major time-varying loads applied to the vanes along the radial direction, becoming responsible for the vane motion during the pumping action. On the basis of this observation, the following subsections provide the analytical procedure developed for their estimation in reference to the vane design parameters and the cam ring profile.

3.1 Vane radial kinematics

The current subsection describes the variable load generated by the vane kinematic motion along the radial direction. Based on Eq. 4, this term is defined as:

$$f_k = -m\ddot{\bar{r}}_G - c\dot{\bar{r}}_G \tag{5}$$

In order to explicit the calculation of this term, it becomes mandatory to determine the kinematic radial motion of the vane. By following the schematic in Fig. 3, the triangle given by points P, O and the center of

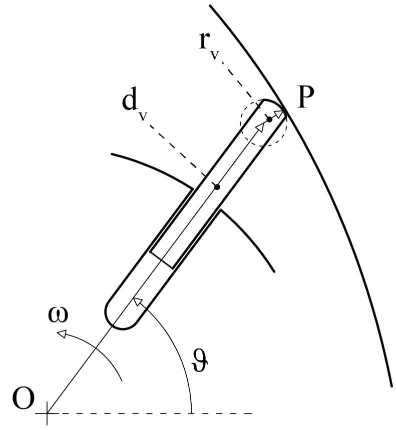

Figure 3: Kinematic representation of the vane cam ring mechanism

the vane tip circle may be used to determine tip circle radial displacement d_v through the cosine theorem:

$$d_v = \sqrt{{r_c}^2 + {r_v}^2 - 2 r_v r_c \cos\left[\tan^{-1}\left(\frac{r'_c|_P}{r_c^{min}}\right)\right]} \tag{6}$$

where r_v represents the vane tip radius, r_c is the cam ring radius and r_c^{min} is its minimum value. Term $r'_c|_P$ indicates the value of the first angular derivative of the cam ring profile at point P. The reader may refer to ref. [17] for a detailed analysis of the pump kinematics.

Equation 6 provides the position of the center of tip circle with respect to the rotor center, for a generic angular position ϑ of the vane, however, based on Eq. 3, the analysis requires the position of vane center of mass r_G. In order to fulfill this purpose, it is worth referring to Fig. 4.a, which details the three main geometrical parameters defining the vane geometry: vane thickness t_v, vane tip radius r_v and vane length l_v. The latter one, in particular, has never been considered in previous analyses, even though it will be shown to play a relevant role in the overall mechanism. By using the auxiliary parameters defined in Fig. 4.b, the following equality is obtained:

$$\bar{r}_G\left[A_r + A_c\right] = \left[d_v + y_0\right] A_c + \left[d_v + \sqrt{{r_v}^2 - (t_v/2)^2} - l_v/2\right] A_r \tag{7}$$

where A_r is the area of the rectangular part of the vane, A_c is the area of the remaining circular segment and y_0 is the distance between the center of the tip circle and the center of mass of the circular segment. It is worth clarifying that all these terms are completely defined by the three parameters in Fig. 4.a :

$$A_c = \frac{{r_v}^2}{2}\left[\sin^{-1}\left(\frac{t_v}{2 r_v}\right) - \frac{t_v}{2 r_v}\right] \tag{8}$$

$$y_0 = \frac{{t_v}^3}{12 A_c} \tag{9}$$

Equations 8 and 9 may be included in Eq. 7 to explicit vane center of mass position r_G:

$$\bar{r}_G = d_v + \frac{{t_v}^3}{12} + t_v\left[\sqrt{{r_v}^2 - (t_v/2)^2} + l_v\right]\left[\sqrt{{r_v}^2 - (t_v/2)^2} - l_v/2\right] \tag{10}$$

Equation 10 provides the position of the vane center of gravity with respect to the pump axis of rotation for each angular position of the vane, known the cam ring profile and the vane geometrical parameters. It is worth noticing that d_v is the only time (or angular) dependent term within the right hand side of the Eq. 10. Therefore, as expected:

$$\dot{\bar{r}}_G = \dot{d}_v = \omega\, {d_v}' \tag{11}$$

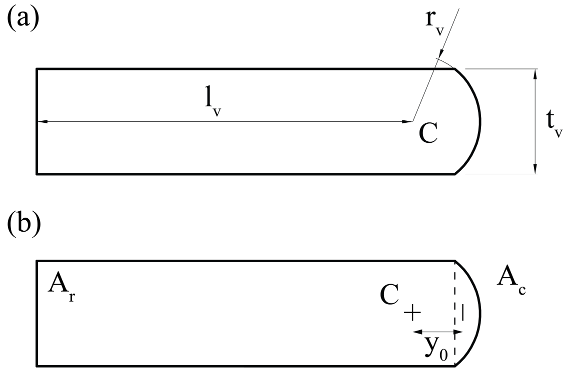

Figure 4: Design parameters defining the vane geometry (a) and auxiliary terms adopted to explicit the radial position of the vane center of mass (b)

while the second derivative becomes:

$$\ddot{\bar{r}}_G = \ddot{d}_v = \omega^2 \; d_v'' \tag{12}$$

in agreement with the hypothesis made in Section 3 that ω is a constant term throughout the entire analysis. The explicit formulation of the first and second derivative of d_v depends on the cam ring profile, therefore, from a practical point of view, their formulation is a consequence of the mathematical law adopted for designing the cam ring.

Based on Eqs. 11 and 12, the kinematic component of the variable loads becomes:

$$f_k = -m\omega^2 \; d_v'' - c\omega \; d_v' \tag{13}$$

which may be further detailed by considering vane material density ρ:

$$f_k = -\rho \; b_v \; \left[t_v \left(\sqrt{{r_v}^2 - (t_v/2)^2} + l_v \right) + \frac{{r_v}^2}{2} \left(\sin^{-1}\left(\frac{t_v}{2r_v}\right) - \frac{t_v}{2r_v} \right) \right] \omega^2 \; d_v'' - c\omega \; d_v' \tag{14}$$

where b_v is the vane facewidth. Equation 14 represents the analytical formulation of the kinematic component of the variable loads applied to each vane along the radial direction, demonstrating that this term mainly depends on the cam ring profile and the vane geometry, while the working condition of the machine, as well as the vane material and the coefficient of friction act as gain parameters.

3.2 Centrifugal force

The present subsection analyses the centrifugal force, which tends to push the vane against the cam ring profile. It is worth noticing that its periodic nature depends on the radial motion of the vane, which actually varies the arm between the rotor center and the vane center of mass. By definition, centrifugal force f_c may be calculated as follows:

$$f_c = -m \; \omega^2 \; (\bar{r}_G + \tilde{r}_G) \tag{15}$$

As a matter of fact, term $\tilde{r}_G$ represents the unknown in the dynamic problem defined by Eq. 4 and therefore the exact calculation of force f_c would not be achievable *a priori*. However, based on the characteristics of the considered mechanism, it is reasonable to assume:

$$|\bar{r}_G| \gg |\tilde{r}_G| \tag{16}$$

since the amplitude of the oscillatory motion generated by the machine dynamics is necessarily some order of magnitude smaller than the mean value of the kinematic radial motion. For the sake of clarity, it has to be underlined that the inequality expressed in Eq. 16 has a general validity, while it does not necessarily apply also to the first and second derivative of the vane radial motion. As a matter of fact, this assumption cannot be referred to vane radial speed and acceleration unless dynamic effects on the vane motion are negligible.

The hypothesis described in Eq. 16 allows to reduce Eq. 15 to:

$$f_c = -m\,\omega^2\,\bar{r}_G \tag{17}$$

which can be straightforwardly expressed with respect to the pump geometrical parameters by using Eq. 10 and the vane material density:

$$\begin{aligned} f_c = -\rho\,\omega^2\,b_v\,\left[t_v\left(\sqrt{{r_v}^2-(t_v/2)^2}+l_v\right)+\frac{{r_v}^2}{2}\left(\sin^{-1}\left(\frac{t_v}{2r_v}\right)-\frac{t_v}{2r_v}\right)\right]\cdot \\ \cdot\left[d_v+\frac{{t_v}^3}{12}+t_v\left(\sqrt{{r_v}^2-(t_v/2)^2}+l_v\right)\left(\sqrt{{r_v}^2-(t_v/2)^2}-l_v/2\right)\right] \end{aligned} \tag{18}$$

As observed regarding the kinematic components of the loads, the periodicity of the centrifugal force is given by term d_v, while all the other factors are determined by the cam ring profile and the vane design parameters.

3.3 Pressure force

The present subsection details the last contribution to the variable loads applied to the vane, which is represented by the pressure force generated by the oil located inside the under-vane pockets. This term has the following general expression:

$$f_p = p\,A \tag{19}$$

where p is the pressure of the oil inside the vane pocket, while A is the area of vane surface facing the oil itself, which is basically defined by vane facewidth b_v multiplied by vane thickness t_v.

Despite pressure force contribution has a straightforward determination apparently, this is actually the term subject to the highest level of uncertainty related to its estimation. The under-vane pockets are small volumes milled from the pump rotor in order to produce a track for the vane displacement. In addition, these pockets are filled by oil with the purpose to enhance the vane motion and promote lubrication between sliding surfaces. The oil filling is usually achieved by dedicated grooves which connect such pockets with the delivery chamber. This solution guarantees the presence of a not-negligible force, i.e. the one defined in Eq. 19, that helps pushing the vane against the cam ring. In this context, it appears to be clear that the estimation of the instantaneous oil pressure inside the pockets constitutes a compelling task, independently whether this purpose is pursued by means of experimental studies of numerical approaches. The former scenario requires to solve a number of technological problems related to the measurement of the pressure of a volume of oil which rotates with the same speed of the pump. An example of this approach may be found in ref. [21], where the authors measured the oil pressure within the pockets of a variable displacement vane pump. The latter scenario, on the other hand, requires the definition of highly detailed Computational Fluid Dynamic models, which are still extremely demanding, both in terms of computational resources and time to reach the solution. Although attainable, it is clear that these methods cannot match with the purposes of the present work, which aims to provide an analytical formulation capable to highlight how the machine behavior is correlated to the main design parameters.

On the basis of these considerations, in the present work the oil pressure within the under-vane pockets has been modeled with Eq. 20, which is widely recognized to satisfactory reproduce pressure variations related to fluid compressibility [4, 8, 13, 19]:

$$\dot{p} = \frac{B}{V}\left[\sum Q - \dot{V}\right] \tag{20}$$

where B is the Bulk's modulus and Q is the generic flow rate entering/leaving the fluid volume. In the assumption that leakages may be negligible with respect to oil volume variation, Eq. 20 reduces to:

$$p(\vartheta) = p_0 - B\int_0^{\vartheta}\frac{V'}{V}d\theta \tag{21}$$

where p_0 is the oil pressure value at the initial reference position and it may be chosen as equal to delivery pressure. Since the integral is known, it is possible to reach the following closed-form solution:

$$p(\vartheta) = p_0 + B\left[\ln V_0 - \ln V(\vartheta)\right] \tag{22}$$

where V_0 is the value of volume V at the initial reference position. The achieved result enlightens the deep correlation between the under-vane pressure force and the volume variation, which is determined by the vane radial motion. As a matter of fact, the volume of under-vane pocket j is given by:

$$V_j(\vartheta) = V_{0j} + b_v\, t_v\, \left[r_G(\vartheta) - r_G(\vartheta = 0)\right] \tag{23}$$

where V_{0j} is the volume of the $j - th$ under-vane pocket at the initial reference position. On the basis of the assumption made in Eq. 16, volume V_j may be calculated as:

$$V_j(\vartheta) = V_{0j} + b_v\, t_v\, \left[d_v(\vartheta) - d_v(\vartheta = 0)\right] \tag{24}$$

A worthwhile choice related to the initial position would be the one defined in Fig. 1, where the $\vartheta = 0$ condition coincides with a vane located on the horizontal line. In this framework, contact point P is on the minimum value of cam ring profile ${r_c}^{min}$ and therefore:

$$V_j(\vartheta) = V_{0j} + b_v\, t_v\, \left[\sqrt{{r_c}^2 + {r_v}^2 - 2r_v r_c \cos\left[\tan^{-1}\left(\frac{r'_c|_P}{r_c^{min}}\right)\right]} - \sqrt{{r_c}^2 + {r_v}^2 - 2r_v r_c}\right] \tag{25}$$

which further reduces to:

$$V_j(\vartheta) = V_{0j} + b_v\, t_v\, \left[\sqrt{{r_c}^2 + {r_v}^2 - 2r_v r_c \cos\left[\tan^{-1}\left(\frac{r'_c|_P}{r_c^{min}}\right)\right]} - r_c + r_v\right] \tag{26}$$

Once the volume variation of a single under-vane pocket has been defined, the correct computation of the pressure force depends on the layout of the pump. In the simplest scenario, the under-vane pockets are disconnected from each others and singularly linked to the outlet chamber. In this context, the oil pressure may be calculated by substituting the definition of V_j into Eq. 22. However, it is worth underlining that more often the pockets are simultaneously exposed to a common chamber, usually milled from the pump cover plates. This chamber basically makes the pockets behave as a unique control volume. Figure 5 provides a schematic representation of the chamber connecting the under-vane pockets. With this layout, the oil pressure needs to be calculated with respect to the volume of the overall chamber, including all the under-vane pockets instantaneously exposed to it:

$$V(\vartheta) = {V_0}^{chamber} + \sum_{j=0}^{n} V_j\left(\vartheta + \frac{2\pi j}{z}\right) \tag{27}$$

where ${V_0}^{chamber}$ is the volume of the chamber connecting the under-vane pockets, n is the number of under-vane pockets linked by the chamber and z is the vane number. It is worth noticing that these two layouts determine time-varying pressure forces with different carrier frequency. In the first scenario, the pressure variation within each under-vane pocket is governed by the periodicity of its own vane radial motion. As a consequence, the carrier frequency is equal to twice the pump rotational frequency. In the latter case, on the contrary, the pressure variation within each under-vane pocket is determined by the superposition of the radial motion of each vane exposed to the common chamber. As a result, the carrier frequency becomes equal to the pump rotational frequency multiplied by the number of vanes, i.e. the carrier frequency of the pumping action.

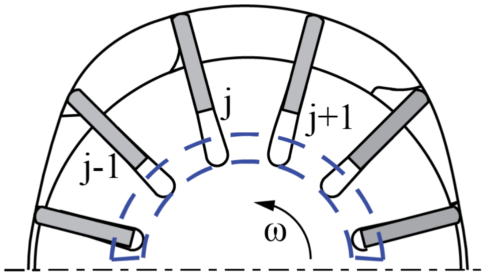

Figure 5: Schematic of the under-vane pockets linked by the common chamber, reported in blue dashed line

4 Result assessment

The current Section provides insights regarding the results that may be obtained from the analytical formulation detailed in Section 3. In addition, the work is focused on analyzing the mutual relationship between the vane geometrical parameters and the time varying loads generated during the vane motion.

In order fulfill this purpose and provide general strength to the achieved results, all the geometrical quantities are defined in nondimensional form (indicated by the $\hat{\cdot}$ symbol) by reporting each parameter as divided by the minimum value of the cam ring radius r_c^{min}. Concurrently, forces are reported in nondimensional form by adopting the following dimensional reduction:

$$\hat{f} = \frac{f}{\rho \, {r_c^{min}}^4 \, \omega^2} \tag{28}$$

which allows to avoid results dependence from pump material and working speed. On the basis of the Buckingham's Theorem [22], the adopted dimensional reduction strategy provides the chance to refer the results to a family of pumps characterized by the same nondimensional specific displacement $\hat{D}_{th}$. As also reported in ref. [13], pump specific displacement may be calculated as:

$$D_{th} = 2\pi \left({r_c^{max}}^2 - {r_c^{min}}^2 \right) \tag{29}$$

where r_c^{max} and r_c^{min} are maximum and minimum value of the cam ring radius, respectively. Based on the proposed dimensional reduction, it is possible to express the nondimensional pump specific displacement as:

$$\hat{D}_{th} = 2\pi \left(\hat{e}^2 - 1 \right) \tag{30}$$

where term $\hat{e}$ is the ratio between r_c^{max} and r_c^{min}. As a consequence, given the values of the specific pump geometrical parameters, the results become valid for the entire set of pumps having the same $\hat{D}_{th}$, independently on their actual size.

The proposed dimensional reduction strategy allows to make a selection on the design parameters that actually have a direct influence on the vane loads and which one is the most appropriate to modify the ratio between each load. However, from a machine design point of view, it is mandatory to investigate the behavior of each force component and why the opportunity to modify their ratio might become a fundamental feature. In order to analyze this aspect, the analytical formulation is applied on a precise family of pumps. Table 1 reports the main design parameters, which satisfy the restrictions related to the vane geometrical admissibility described in ref. [17]. The resulting cam ring profile is obtained with a 5^{th} order polynomial law. By assuming $\hat{p}_0 = 0.1$, $\hat{B} = 1600$, $\zeta = 0.1$ and $\Omega = 2$, the reference pump design leads to the four load components in Fig. 6, where the term $\hat{f}_k$ has been divided in two contributions, i.e. force $\hat{f}_k^a$ and force $\hat{f}_k^v$. The four parameters assumed for obtaining the forces in Fig. 6 come from typical working conditions of this kind of machines and they do not alter the actual behavior of each force component.

Fig. 6 provides the chance to analyze how each load is characterized by a peculiar behavior. The centrifugal force is strictly positive, being proportional to vane displacement. As a consequence, this load constantly

Table 1: Pump design parameters in nondimensional form

z	10
$\hat{e}$	$\sqrt{1+1/2\pi}$
$\hat{r}_v$	0.3
$\hat{t}_v$	0.1
$\hat{l}_v$	$0.5\ \hat{e}$
ϑ_{SR}	$\pi/10$
ϑ_{ER}	$2\pi/5$
ϑ_{SF}	$3\pi/5$
ϑ_{EF}	$9\pi/10$

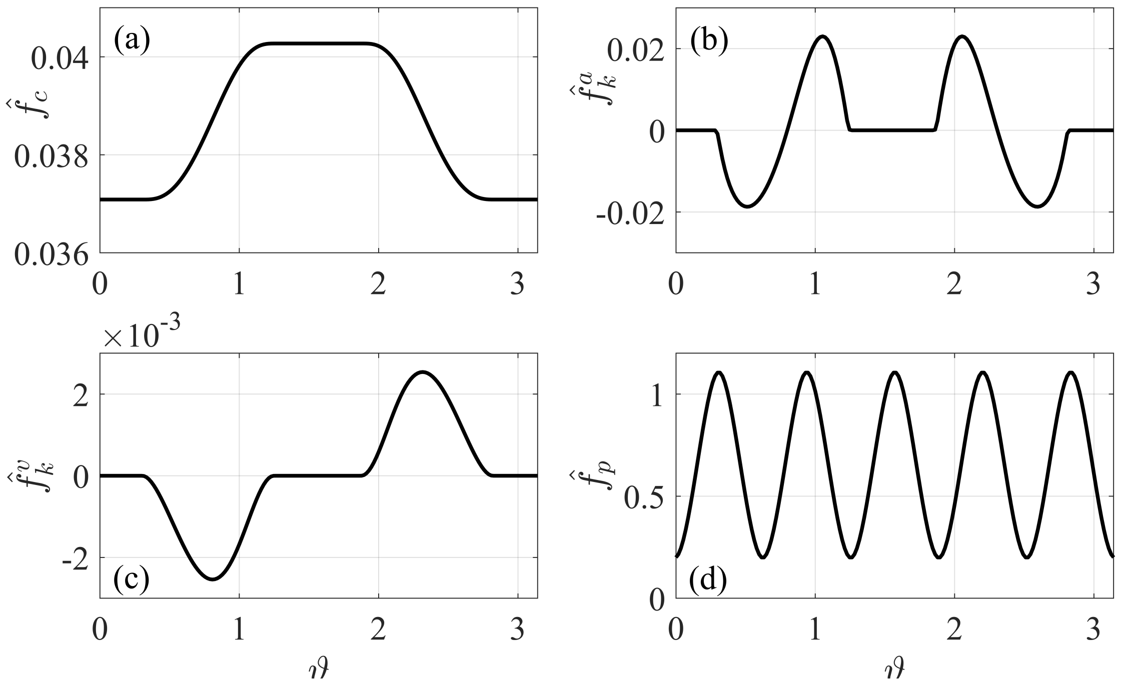

Figure 6: Schematic of the under-vane pockets linked by the common chamber, reported in blue dashed line

helps pushing the vane against the cam ring and its magnitude increases during the rise phase, while it decreases during fall phase. A similar contribution is provided by force $\hat{f}_p$, which is strictly positive and it shows a periodic fluctuation with a carrier frequency defined by the vane passage frequency. It is worth noticing that, despite the magnitude of this load appears to make all the other contributions irrelevant, this result depends on the chosen parameter $\hat{p}_0$ and $\hat{B}$, which are affected by a quadratic decrease as the pump speed increases linearly. Finally, a peculiar role is addressed by force components $\hat{f}_k^a$ and $\hat{f}_k^v$, which show an alternating behavior as a direct consequence of the kinematic radial motion of the vane. Force $\hat{f}_k^v$ is negative during the rise phase while it switches to positive values within the fall phase. On the other hand, force $\hat{f}_k^a$ oscillates through negative and positive values within each rise and fall phase. During the dwell phases, both $\hat{f}_k^a$ and $\hat{f}_k^v$ are equal to zero. As noticed regarding force $\hat{f}_p$, it has to be underlined that although $\hat{f}_k^a$ only depends on the pump geometry, force $\hat{f}_k^v$ increases as the pump speed is reduced. Based on this analysis, it may be clearly recognized that forces $\hat{f}_k^a$ and $\hat{f}_k^v$ are detrimental components for the correct machine operation since they tends to unload the vane promoting its detachment from the cam ring profile. This phenomenon is a catastrophic but realistic risk for this kind of volumetric pumps, as also recognized in ref.

[15], and therefore the capability to control the vane loads during the machine design phase may represent a successful competence.

5 Concluding remarks

The proposed study provides an analytical dissertation regarding the determination of the vane radial loads in balanced vane pumps. The methodology allows to calculate the main vane radial load components, i.e. centrifugal, inertia and damping and pressure force, on the basis of a kinetostatic approach. Within this context, the method allows to include the influence of a large variety of design parameters, involving both vane geometry and cam ring profile.

In order to assess the capabilities of the provided analytical formulation, a dedicated assessment of the results has been performed. Within this context, a dimensional reduction strategy based on the Buckingham's Theorem has been applied to the formulation of each load component. The proposed dimensional reduction strategy helps making a selection on the design parameters that actually have a direct influence on the vane loads and which one is the most appropriate to modify the ratio between each load. In order to analyze this aspect, the analytical formulation has been applied on a precise family of pumps.

As a concluding remark, the present study has demonstrated the existence of a deep correlation between the pump geometrical parameters and the kinetostatic radial loads applied to the vanes. Within this framework, the provided analytical dissertation is capable to isolate the links between the load components and each design parameter, providing practical insights regarding the correct balancing the vane and the feasibility of the pump design.

References

[1] W. Wilson, "Rotary-pump theory," *Transaction of the ASME*, no. 4, pp. 371–384, 1946.

[2] W. Wilson, "Clearance design in positive-displacement pumps," *Machine Design*, no. 2, pp. 127–130, 1953.

[3] C. Bonacini, "Sulla portata delle pompe a ingranaggi," *L'Ingegnere*, vol. 9, 1961.

[4] A. Vacca and M. Guidetti, "Modelling and experimental validation of external spur gear machines for fluid power applications," *Simulation Modelling Practice and Theory*, vol. 19, no. 9, pp. 2007 – 2031, 2011.

[5] M. Battarra and E. Mucchi, "On the assessment of lumped parameter models for gear pump performance prediction," *Simulation Modelling Practice and Theory*, vol. 99, p. 102008, 2020.

[6] E. Mucchi, G. Dalpiaz, and A. F. del Rincòn], "Elastodynamic analysis of a gear pump. part i: Pressure distribution and gear eccentricity," *Mechanical Systems and Signal Processing*, vol. 24, no. 7, pp. 2160 – 2179, 2010.

[7] R. Frith and W. Scott, "Comparison of an external gear pump wear model with test data," *Wear*, vol. 196, no. 1, pp. 64 – 71, 1996.

[8] M. Rundo, "Models for flow rate simulation in gear pumps: a review," *Energies*, vol. 10, no. 9, p. 1261, 2017.

[9] L. Olems, "Investigations of the temperature behaviour of the piston cylinder assembly in axial piston pumps," *International Journal of Fluid Power*, vol. 1, no. 1, pp. 27–39, 2000.

[10] A. Schenk and M. Ivantysynova, "A Transient Thermoelastohydrodynamic Lubrication Model for the Slipper/Swashplate in Axial Piston Machines," *Journal of Tribology*, vol. 137, no. 3, 07 2015.

[11] A. M. Karmel, "A Study of the Internal Forces in a Variable-Displacement Vane-Pump - Part I: A Theoretical Analysis," *Journal of Fluids Engineering*, vol. 108, no. 2, pp. 227–232, 06 1986.

[12] A. M. Karmel, "A Study of the Internal Forces in a Variable-Displacement Vane-Pump - Part II: A Parametric Study," *Journal of Fluids Engineering*, vol. 108, no. 2, pp. 233–237, 06 1986.

[13] J. Ivantysyn and M. Ivantysynova, *Hydrostatic pumps and motors*. Academia Books International, 2001.

[14] K. Hattori, H. Suzuki, and H. J, "Design method of small-ripple vane pumps," *SAE Technical paper*, no. 871681, pp. 83–90, 1987.

[15] M.-R. Cho and D.-C. Han, "Vane tip detachment in a positive-displacement vane pump," *KSME International Journal*, vol. 12, no. 5, pp. 881–887, 1998.

[16] Y. Inaguma and N. Yoshida, "Variation in driving torque and vane friction torque in a balanced vane pump," *SAE Technical paper*, no. 1764, 2014.

[17] M. Battarra, A. Blum, and E. Mucchi, "Kinematics of a balanced vane pump with circular tip vanes," *Mechanism and Machine Theory*, vol. 137, pp. 355 – 373, 2019.

[18] M. Battarra and E. Mucchi, "On the relation between vane geometry and theoretical flow ripple in balanced vane pumps," *Mechanism and Machine Theory*, vol. 146, p. 103736, 2020.

[19] M. Battarra and E. Mucchi, "A method for variable pressure load estimation in spur and helical gear pumps," *Mechanical Systems and Signal Processing*, vol. 76–77, pp. 265–282, 2016.

[20] M. Buzzoni, M. Battarra, E. Mucchi, and G. Dalpiaz, "Motion analysis of a linear vibratory feeder: dynamic modeling and experimental verification," *Mechanism and Machine Theory*, vol. 114, pp. 98–110, 2017.

[21] E. Mucchi, G. Cremonini, S. Delvecchio, and G. Dalpiaz, "On the Pressure Ripple Measurement in Variable Displacement Vane Pumps," *Journal of Fluids Engineering*, vol. 135, no. 9, 06 2013.

[22] E. S. Taylor, *Dimensional analysis for engineers*. Oxford University Press, 1974.